

Low-temperature heat transport in the layered spin-dimer compound $\text{Ba}_3\text{Mn}_2\text{O}_8$

W. P. Ke,¹ X. M. Wang,¹ C. Fan,¹ Z. Y. Zhao,¹ X. G. Liu,¹ L. M. Chen,² Q. J. Li,¹ X. Zhao,³ and X. F. Sun^{1,*}

¹Hefei National Laboratory for Physical Sciences at Microscale, University of Science and Technology of China, Hefei, Anhui 230026, People's Republic of China

²Department of Physics, University of Science and Technology of China, Hefei, Anhui 230026, People's Republic of China

³School of Physical Sciences, University of Science and Technology of China, Hefei, Anhui 230026, People's Republic of China

(Received 15 April 2011; revised manuscript received 26 July 2011; published 23 September 2011)

We report a study on the low-temperature heat transport of the $\text{Ba}_3\text{Mn}_2\text{O}_8$ single crystal, a layered spin-dimer compound exhibiting the magnetic-field-induced magnetic order or the magnon Bose-Einstein condensation. The thermal conductivities (κ) along both the ab plane and the c axis show nearly isotropic dependence on magnetic field; that is, κ is strongly suppressed with increasing field, particularly at the critical fields of magnetic phase transitions. These results indicate that the magnetic excitations play a role of scattering phonons and the scattering effect is enhanced when the magnetic field closes the gap in the spin spectrum. In addition, the magnons in the BEC state of this material do not show notable ability of carrying heat.

DOI: 10.1103/PhysRevB.84.094440

PACS number(s): 66.70.-f, 75.47.-m, 75.50.-y

I. INTRODUCTION

Low-dimensional or frustrated quantum magnets were revealed to exhibit exotic ground states, magnetic excitations, and quantum phase transitions (QPTs).^{1,2} For a particular case of the spin-gapped antiferromagnets, the external magnetic field can close the gap in the spectrum, which results in a QPT between a low-field disordered paramagnetic phase and a high-field long-range ordered one. An intriguing finding is that this ordered phase can be approximately described as a Bose-Einstein condensation (BEC) of magnons.³ Many experimental investigations on the critical properties of the BEC-related QPT have been carried out, including the characterizations of the magnon spectrum, the magnetization, the specific heat, and the thermal transport.³ In a recent study, the heat transport properties of a magnon BEC material, $\text{NiCl}_2\text{-}4\text{SC}(\text{NH}_2)_2$ (DTN), were found to display strong anomalies at the QPTs and the heat conductivity of the BEC state seemed to be much enhanced upon lowering temperatures (approaching the absolute zero).⁴ This result shows an analogy between the magnon BEC and the superfluid of ^4He in the aspect of the ability of transporting heat. However, one notable facet is that magnons act as heat carriers only in the direction of the spin chains of this compound, whereas they only scatter phonons in the transverse direction.⁴ So the exchange anisotropy may play the key role in the heat transport of magnetic excitations. A later experimental work confirmed the main features of transport properties of DTN, but an alternative picture based on the mass renormalization and impurity scattering effects was proposed to explain the thermal transport data.⁵ In any case, the QPTs associated with the magnon BEC are believed to significantly affect the heat transport properties and the low-energy magnetic excitations provide a substantial contribution to the heat transport. To get the general principals of the heat transport in the magnon BEC state, we need to carry out systematic studies on more members of the magnon BEC materials.

$\text{Ba}_3\text{Mn}_2\text{O}_8$ (BMO) is an $S=1$ quantum spin-dimer system exhibiting the BEC of spin degrees of freedom. It crystallizes in the rhombohedral $R\bar{3}m$ structure with the pairs of $\text{Mn}^{5+} 3d^2$ ions ($S=1$) arranged vertically on the hexagonal

layers.⁶ The spins of Mn^{5+} ions of each pair are coupled antiferromagnetically to form spin dimers.⁷⁻⁹ Neutron scattering results indicated an intradimer exchange energy $J_0=1.642$ meV, an interdimer coupling between Mn ions in the same plane $J_2 - J_3=0.1136$ meV, an interdimer coupling between Mn ions in the adjacent planes $J_1=-0.118$ meV, and the next nearest neighbor interdimer interactions between bilayers (along the c axis) $J_4=-0.037$ meV.¹⁰⁻¹⁴ The strong in-plane spin-dimer interaction results in a spin-singlet ground state, with a spin gap of 1.05 meV to the lowest triplet state and a second larger gap to the quintuplet state. BMO displays a peculiar phase diagram in magnetic field when the Zeeman effect lowers the $S_Z=1$ triplet states and the $S_Z=2$ quintuplet states.¹³ Corresponding to the closures of two spin gaps with increasing magnetic field, there are two sequential magnetically ordered states and four quantum critical fields: $H_{c1}=8.7$ T, $H_{c2}=26.5$ T, $H_{c3}=32.5$ T, $H_{c4}=47.9$ T for $H \parallel c$.^{7,12,13} The peculiarity is that the first ordered phase for $H_{c1} < H < H_{c2}$ and the second one for $H_{c3} < H < H_{c4}$ are described as the triplet condensation and the quintuplet condensation, respectively.¹³ Furthermore, BMO was found to have a weak single-ion uniaxial anisotropy, characterized by $|D|=0.032$ meV.¹⁴ The phase diagram for $H \perp c$ is a bit more complicated, with two phases of the triplet condensation.¹²⁻¹⁴ It was revealed that both the single-ion anisotropy and the geometry frustration play crucial roles in determining the phase diagram.¹²

In this work, we study the thermal conductivity (κ) of the BMO single crystal to probe the field-induced QPTs and the role of magnetic excitations in the heat transport. It is found that both κ_{ab} and κ_c are strongly suppressed in magnetic fields, particularly at the field-induced QPTs, which demonstrates that at very low temperatures the magnons mainly act as phonon scatterers even in the long-range ordered state. The present results indicate that the magnon-BEC state may not necessarily exhibit large thermal conductivity and the ability of magnetic excitations transporting heat is determined by the magnetic structure and the anisotropic spin exchange.

II. EXPERIMENTS

High-quality single crystals of $\text{Ba}_3\text{Mn}_2\text{O}_8$ are grown by a slow-cooling method using NaOH as a solvent.¹² The crystals have a hexagonal-platelet-like shape with large sizes up to $5 \times 5 \times 2.5 \text{ mm}^3$. The largest surface is the ab plane and the thickness is along the c axis, determined by using the x-ray diffraction and the Laue photograph. The specific heat is measured by the relaxation method in the temperature range from 0.4 to 20 K using a commercial physical property measurement system (PPMS, Quantum Design). Both the ab plane and the c axis thermal conductivities (κ_{ab} and κ_c) are measured using the conventional steady-state technique. Particularly, the data at low temperature and in high magnetic field are taken by using a “one heater, two thermometer” method in a ^3He refrigerator and a 14 T magnet.^{4,15,16} Note that we can only probe the QPTs at the first critical field of BMO, due to the limitation of the available field.

III. RESULTS AND DISCUSSION

It is known that, in a magnetic insulator, heat can be carried by phonons and magnetic excitations, and the interaction between them usually induces scattering on heat carriers, which is a negative effect on the heat transport. To analyze the heat transport properties quantitatively, it is necessary to know the phononic specific heat from the experiments. Figure 1 shows the low- T specific heat of the $\text{Ba}_3\text{Mn}_2\text{O}_8$ single crystal. At ~ 6 K, there appears a broad shoulder-like feature, which is apparently of magnetic origin. Below 5 K, the specific heat decreases quickly with temperature and it does not show a T^3 dependence of the phonon specific heat. The same result has been reported in an earlier work.⁸ The low- T specific heat was found to be able to be described by a formula for the gapped magnetic excitations,⁸

$$C = \tilde{n}R(\Delta/T)^2 e^{-\Delta/T}, \quad (1)$$

where \tilde{n} is the number of excited states per spin dimer, R is the gas constant, and Δ is the energy gap of magnetic

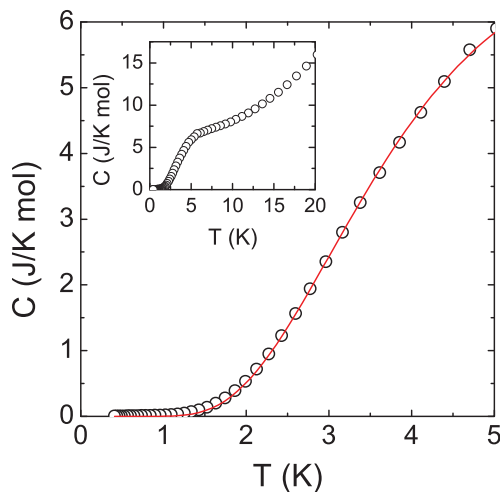


FIG. 1. (Color online) Low-temperature specific heat of $\text{Ba}_3\text{Mn}_2\text{O}_8$ single crystal in zero field. The solid line indicates the fit of data using formula (1). Inset: The data in a broader temperature range from 0.4 to 20 K.

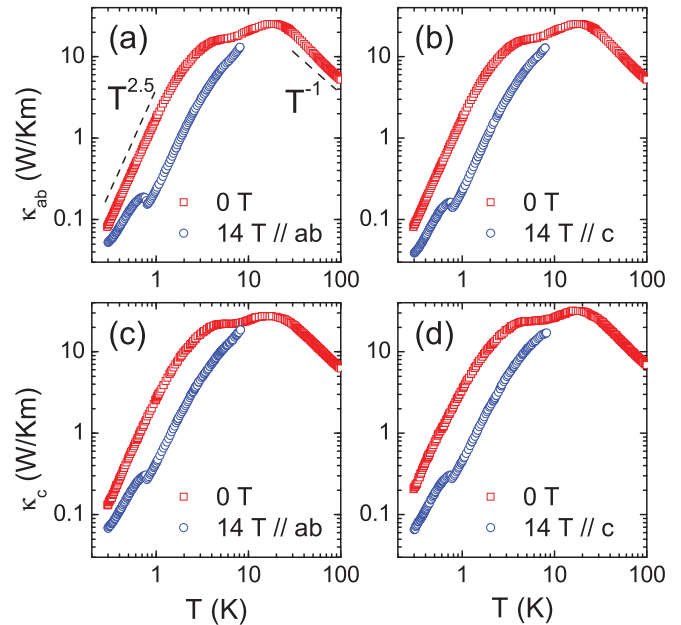


FIG. 2. (Color online) Temperature dependencies of the thermal conductivities κ_{ab} and κ_c of $\text{Ba}_3\text{Mn}_2\text{O}_8$ single crystals in zero and 14 T fields. The dashed lines indicate the approximate $T^{2.5}$ and T^{-1} dependencies of the thermal conductivity at very low temperatures and at high temperatures, respectively.

excitations. The low- T data can be fitted rather well to Eq. (1) with parameters $\tilde{n} = 1.49$ and $\Delta = 14.2$ K, except for the very low T data (< 1 K).⁸ Note that the size of the gap is quite consistent with those from other measurements.^{7,11} However, it is difficult to separate the phononic specific heat because of the significant contribution from the magnetic excitations. Actually, adding a T^3 term to Eq. (1) cannot achieve perfect fitting to the data, particularly for the sub-Kelvin data.

Figure 2 shows the temperature dependencies of κ_{ab} and κ_c of BMO single crystals in zero and 14 T fields, which are applied along either the ab plane or the c axis. Apparently, the zero-field thermal conductivities show rather weak anisotropy at high temperatures. Each $\kappa(T)$ curve exhibits a phonon peak at 18 K with the peak values nearly the same for κ_{ab} and κ_c . The T^{-1} dependence of $\kappa(T)$ at high temperatures is the characteristic of phonon heat transport dominated by the phonon-phonon Umklapp scattering.¹⁷ At sub-Kelvin temperatures, both $\kappa_{ab}(T)$ and $\kappa_c(T)$ show an approximate $T^{2.5}$ dependence, which indicates that the boundary scattering limit of phonon thermal conductivity is approached or that the microscopic scattering on phonons is negligible.¹⁷ Besides these usual behaviors belonging to the phonon heat transport, there is a “shoulder-like” feature in the zero-field $\kappa(T)$ at 6.5 K, which is likely due to some kind of resonant scattering on phonons.¹⁷ Applying 14 T magnetic field leads to a strong suppression of low- T thermal conductivity and the disappearance of the shoulder-like feature. Therefore, the phonon resonant scattering in zero field must be of magnetic origin. A similar result has been found in another spin-gapped material, DTN.⁴ On the other hand, there is no evidence for the magnon heat transport in BMO, which is reasonable at very low temperatures considering the negligible magnon

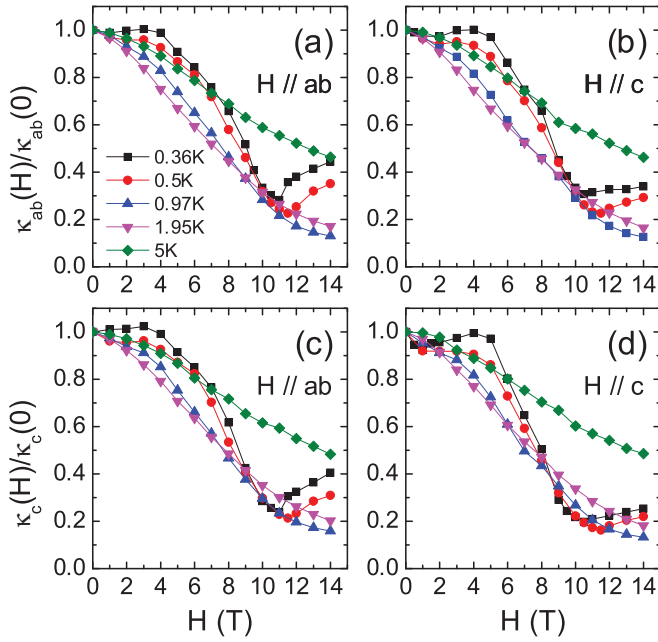


FIG. 3. (Color online) Magnetic-field dependencies of thermal conductivity of $\text{Ba}_3\text{Mn}_2\text{O}_8$ single crystals at low temperatures.

excitations due to the finite spin gap. In high magnetic field, the strong suppression of phonon heat transport in a broad temperature range is apparently due to the enhancement of magnetic scattering, which can also be seen from the following magnetic-field dependencies of κ . Another peculiar feature of 14 T $\kappa(T)$ data is the small jumps of conductivity at low temperatures, which are related to the field-induced antiferromagnetic (AF) transitions. Note that even with these increases of κ at the phase transitions, the lower T thermal conductivities are still much smaller than the zero-field values, indicating that the phonons are still strongly scattered by magnetic excitations in the field-induced AF state.

Figure 3 shows the detailed magnetic field dependencies of κ_c and κ_{ab} for both $H \parallel ab$ and $H \parallel c$. It is clear that they are nearly isotropic on the field direction. The overall behavior of $\kappa(H)$ is that the magnetic field strongly suppresses thermal conductivity, but at very low temperatures; i.e., at 0.36 and 0.5 K, κ shows upturn above some critical fields. Since the zero-field thermal conductivity of BMO is purely phononic, the field-induced suppression of κ is clearly a result of the scattering effect on phonons by some magnetic excitations. In this regard, the phonon scattering by paramagnetic moments, which are commonly existing as impurities or spin vacancies, is one of the unavoidable effects.^{17–19} However, the field dependencies of κ shown in Fig. 3 are rather different from the standard one of paramagnetic moment scattering.^{17,18} The main origin for the $\kappa(H)$ behaviors is therefore the phonon scattering by magnon excitations. The low-field quantum disordered phase has a finite spin gap, which can be weakened by the Zeeman effect. At a fixed temperature, with increasing the magnetic field, the spin gap decreases and the number of low-energy magnons increases quickly, which can strongly scatter phonons and leads to a significant suppression of κ .

A notable feature of $\kappa(H)$ isotherms is the upturn of κ in high magnetic field and at very low temperatures. This

increase of κ is obviously related to the field-induced AF order since the transition fields are found to coincide with the phase boundary of the high-field ordered phase, i.e., the magnon BEC state. There are two possible reasons for the increase of κ in the BEC state. First, the phonon scattering by magnons is weakened when the magnon BEC occurs. Second, the magnons in the BEC state have a positive effect on κ by transporting the heat directly. If the magnons transport the energy, due to the anisotropy of the exchange and the low-dimensionality of the spin structure, the field dependence of κ should exhibit obvious anisotropy on the direction of heat current with the same field.^{20–22} However, it can be seen from Fig. 3 that the upturn behaviors actually show a weak anisotropy on the direction of magnetic field rather than on that of the heat current. This means that the upturn of thermal conductivity in the BEC state is a result of the weakening of magnon-phonon scattering. In other words, although the magnon scattering on phonons is generally strong at high fields, it is more significant at the critical fields because of the strong spin fluctuations.

Although the above discussions are quite clear in catching the main physics of the observed heat transport properties, it is useful to try a more quantitative analysis on the experimental data. First, since the phonons are the only type of heat carrier, the zero-field $\kappa(T)$ data are likely to be fitted by a classical Debye model of phonon thermal conductivity,^{17,23}

$$\kappa_{ph} = \frac{k_B}{2\pi^2 v} \left(\frac{k_B}{\hbar} \right)^3 T^3 \int_0^{\Theta_D/T} \frac{x^4 e^x}{(e^x - 1)^2} \tau(\omega, T) dx, \quad (2)$$

in which ω is the phonon frequency, $x = \hbar\omega/k_B T$ is dimensionless, and $1/\tau(\omega, T)$ is the phonon relaxation rate. The relaxation time is determined by

$$\tau^{-1} = \nu/L + A\omega^4 + B T \omega^3 \exp(-\Theta_D/bT) + \tau_{res}^{-1}, \quad (3)$$

which represent the phonon scattering by the grain boundary, the point defects, the phonon-phonon Umklapp scattering, and the resonant scattering, respectively.¹⁷ The average sound velocity ν can be calculated from the Debye temperature using the formula $\Theta_D = \nu(\hbar/k_B)(6\pi^2 n)^{1/3}$, where n is the number density of atoms. For BMO, however, the Debye temperature cannot be simply obtained from the phonon specific-heat data, as the data in Fig. 1 indicate. For an estimation, we refer to the specific-heat data of $\text{Ba}_3\text{V}_2\text{O}_8$,²⁴ a nonmagnetic material having the same crystal structure as BMO. The phonon specific-heat coefficient $\beta = 6.06 \times 10^{-4} \text{ J/K}^4 \text{ mol}$ can be easily obtained from a T^3 fitting to the low- T data.²⁴ With this β value, the Debye temperature and the sound velocity of BMO are calculated to be 346 K and 2900 m/s, respectively. The parameter L describing the boundary scattering is the averaged sample width of the samples. The other parameters A , B , and b are free ones.

One difficulty of getting a precise calculation using Eq. (2) is the description of τ_{res}^{-1} . In BMO, the magnetic excitations can strongly scatter phonons. Considering the energy dispersion of magnons, it is very difficult to get a transparent formula for τ_{res}^{-1} . For a simple analysis, one can neglect the magnon dispersion and assume that the resonant scattering of phonons

occurs via a singlet-triplet excitations of dimerized states. Thus, the resonant scattering rate can be expressed as

$$\tau_{\text{res}}^{-1} = C \frac{\omega^4}{(\omega_0^2 - \omega^2)^2} F(T), \quad (4)$$

where C is a free parameter while $F(T)$ describes the difference of thermal populations of the excited triplet and the ground singlet states (the contribution of a higher level excitation of quintuplet states is negligibly small). It is known that^{11,23}

$$F(T) = 1 - \frac{1 - \exp(-\Delta/T)}{1 + 3 \exp(-\Delta/T)}, \quad (5)$$

with $\Delta = \hbar\omega_0$ the energy gap of magnetic spectrum, which is about 14.2 K from the specific-heat data.

The zero-field thermal conductivity data are able to be fitted by using the above formula very well. As an example, the zero-field data from Fig. 2(a) and the fitting curve are displayed in Fig. 4(a). The best-fitting parameters are $A = 1.3 \times 10^{-42} \text{ s}^3$, $B = 3.0 \times 10^{-30} \text{ K}^{-1} \text{ s}^2$, $b = 6.0$, and $C = 1.6 \times 10^8 \text{ s}^{-1}$.

Second, the magnetic-field dependence of κ can also be calculated using the Debye model. The effect of magnetic field is to induce the Zeeman splitting of the degenerate triplet states and a linear decrease of the energy gap with field; that is,

$$\Delta(H) = \Delta - g\mu_B H/k_B. \quad (6)$$

The Landé factor was known to be ~ 2.00 .^{11,12} A typical comparison between the $\kappa(H)$ data and the calculations is

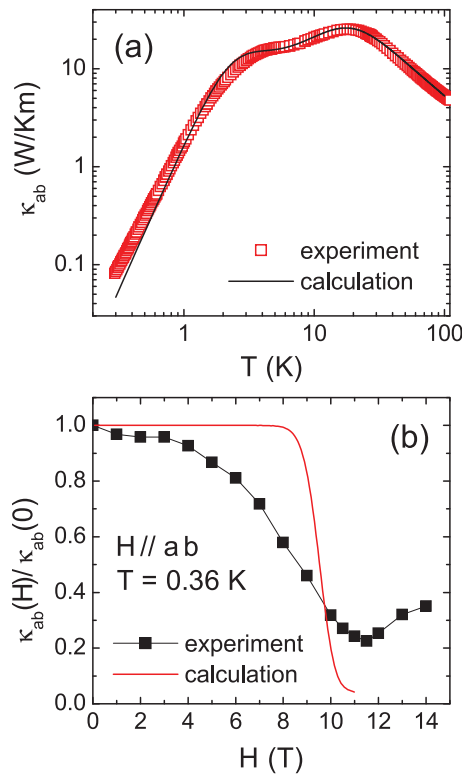


FIG. 4. (Color online) Comparison of the $\kappa_{ab}(T)$ data (a) and the $\kappa_{ab}(H)$ data (b) with the calculation results using the Debye model.

shown in Fig. 4(b). Although there is a qualitative agreement between the experimental data and the calculation, the quantitative difference is quite large. In particular, at low fields the experimental data show much stronger suppression than the calculated result. It is expected from the classical Boltzmann distribution that the magnon excitations are negligibly weak at sub-Kelvin temperatures when the spin gap is larger than 10 K. The experimental data suggest that the magnon excitations, which may be because of the quantum fluctuations, are much stronger than the thermal excitation produces. Another reason for the significant discrepancy is likely related to the simple assumption of the resonant phonon scattering by the two-level magnetic excitations. Actually, the magnon dispersions of BMO are not very weak, which makes the scattering between phonons and magnetic excitations inelastic and much more complicated. A precise calculation based on the magnon-phonon scattering calls for the details of both the phonon spectra and the magnon dispersions.^{25,26}

It is useful to compare these results with those of DTN, in which the magnetic field along the c axis (the spin-chain direction) can close the spin gap and drive the AF phase transition. In DTN, the heat transport along the c axis or perpendicular to it presents remarkably anisotropic behaviors with increasing field; that is, κ_c show sharp peaks at H_{c1} while κ_{ab} show dips at the same position.⁴ Those demonstrated that magnons act as the heat carriers along the c axis and the phonon scatterers along the ab plane, respectively.⁴ Furthermore, the κ_c of DTN in the AF state (for $H_{c1} < H < H_{c2}$) keep increasing with lowering the temperature, also pointing to a potentially large heat transport in the magnon BEC phase.^{4,5} The present $\kappa(H)$ behaviors of BMO for both κ_{ab} and κ_c are very similar to those of $\kappa_{ab}(H)$ in DTN, which suggests that the magnetic scattering

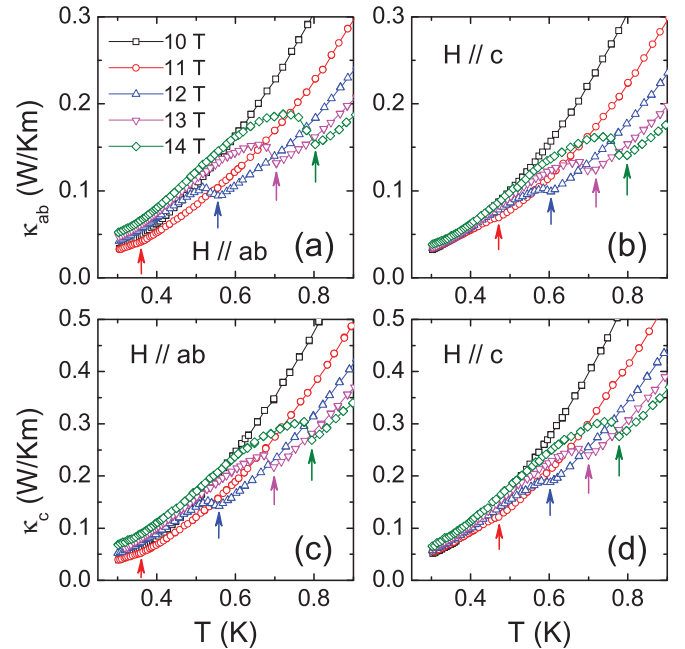


FIG. 5. (Color online) Temperature dependencies of the thermal conductivity measured in magnetic field above the critical field H_{c1} . The arrows indicate the critical temperatures where κ starts to increase.

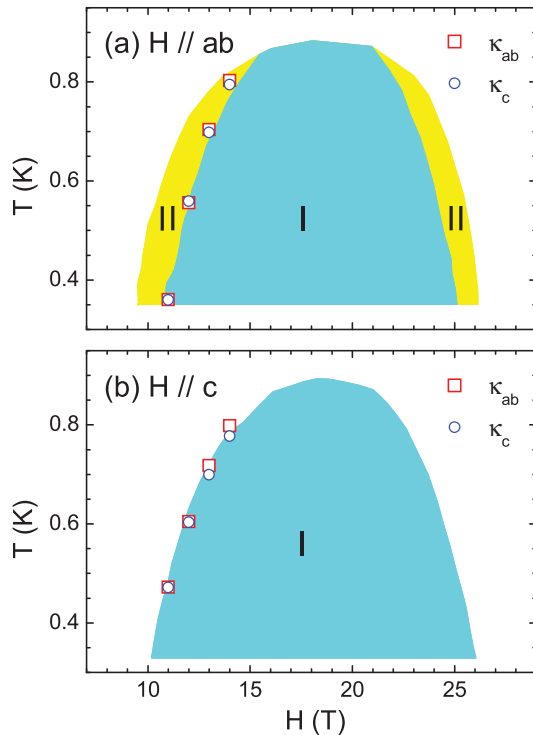


FIG. 6. (Color online) The transition points of $\kappa(T)$ curves from Fig. 3. Temperature-field phase diagram, obtained by heat capacity and magnetocaloric effect measurements from Ref. 12, is shown for comparison. I and II indicate two different phases of the triplet condensate (Ref. 12).

on phonons is enhanced upon approaching the critical fields. In contrast to the case of DTN, the magnetic excitations of BMO do not contribute to transporting heat substantially along either the ab plane or the c axis. Therefore, whether the magnon BEC state of the spin-gapped compounds can have strong ability of transporting heat is mainly dependent on such factors as the nature of the magnetic structure and the exchange anisotropy. The field-induced AF state or magnon BEC is not the sufficient condition for observable magnon transport.

The above are, however, not the whole story because there is only one transition in each $\kappa(H)$ isotherm for both $H \parallel c$ and $H \parallel ab$, whereas the former experiments revealed a single magnetic transition and two distinct transitions, respectively. For more precise description, we show in Fig. 5 a series

of $\kappa(T)$ curves for magnetic fields varying between 10 and 14 T. It is found that below 10 T, there is no anomaly in the $\kappa(T)$ curves down to 0.3 K. Above 10 T, a jump in $\kappa(T)$ shows up and becomes bigger with increasing field up to 14 T. From these data, we can obtain the transition points on the H - T phase diagram and compare them with the boundaries of the magnetically ordered phases determined by heat capacity, magnetocaloric effect, and cantilever torque measurements,¹² as shown in Fig. 6. It is interesting that the jumplike anomalies of κ occur at the boundary of phase I; that is, the thermal conductivity increases at the phase transitions to phase I from either the low-field disordered state or the antiferromagnetically ordered phase II. This phenomenon has a good correspondence to the specific-heat data,¹² which show a sharp lambda-like peak and a much weaker and less divergent peak at the phase transitions from the disordered state or phase II to phase I and the disordered state to phase II, respectively. It is likely that the phase transition associated with lambda-like specific-heat anomaly has more significant critical fluctuations that strongly scatter phonons.

IV. SUMMARY

We study the heat transport of $\text{Ba}_3\text{Mn}_2\text{O}_8$ single crystals at very low temperatures and in high magnetic fields to probe the field-induced magnetic phase transitions and the role of magnons in the transport properties. In zero field, the low- T thermal conductivity shows a purely phononic transport behavior. In applied strong field, the spin gap is gradually diminished and the magnetic excitations are populated, which induces an enhanced magnetic scattering on phonons and an overall strong suppression of thermal conductivity with increasing field. Moreover, at very low temperatures where the closure of the spin gap results in a long-range ordered AF state, the phonons are more significantly scattered at the phase transitions. There is no evidence showing sizable magnetic heat transport in this magnon BEC compound.

ACKNOWLEDGMENTS

This work was supported by the Chinese Academy of Sciences, the National Natural Science Foundation of China, and the National Basic Research Program of China (Grants No. 2009CB929502 and No. 2011CBA00111).

*xfsun@ustc.edu.cn

¹S. Sachdev, *Nature Phys.* **4**, 173 (2008), and references therein.

²L. Balents, *Nature (London)* **464**, 199 (2010).

³For a review, see T. Giamarchi, C. Rüegg, and O. Tchernyshyov, *Nature Phys.* **4**, 198 (2008).

⁴X. F. Sun, W. Tao, X. M. Wang, and C. Fan, *Phys. Rev. Lett.* **102**, 167202 (2009).

⁵Y. Kohama, A. V. Sologubenko, N. R. Dilley, V. S. Zapf, M. Jaime, J. A. Mydosh, A. Paduan-Filho, K. A. Al Hassanieh, P. Sengupta,

S. Gangadharaiah, A. L. Chernyshev, and C. D. Batista, *Phys. Rev. Lett.* **106**, 037203 (2011).

⁶M. Uchida, H. Tanaka, M. I. Bartashevich, and T. Goto, *J. Phys. Soc. Jpn.* **70**, 1790 (2001).

⁷M. Uchida, H. Tanaka, H. Mitamura, F. Ishikawa, and T. Goto, *Phys. Rev. B* **66**, 054429 (2002).

⁸H. Tsujii, B. Andraka, M. Uchida, H. Tanaka, and Y. Takano, *Phys. Rev. B* **72**, 214434 (2005).

⁹B. Xu, H. T. Wang, and Y. P. Wang, *Phys. Rev. B* **77**, 014401 (2008).

- ¹⁰M. B. Stone, M. D. Lumsden, Y. Qiu, E. C. Samulon, C. D. Batista, and I. R. Fisher, *Phys. Rev. B* **77**, 134406 (2008).
- ¹¹M. B. Stone, M. D. Lumsden, S. Chang, E. C. Samulon, C. D. Batista, and I. R. Fisher, *Phys. Rev. Lett.* **100**, 237201 (2008).
- ¹²E. C. Samulon, Y.-J. Jo, P. Sengupta, C. D. Batista, M. Jaime, L. Balicas, and I. R. Fisher, *Phys. Rev. B* **77**, 214441 (2008).
- ¹³E. C. Samulon, Y. Kohama, R. D. McDonald, M. C. Shapiro, K. A. Al-Hassanieh, C. D. Batista, M. Jaime, and I. R. Fisher, *Phys. Rev. Lett.* **103**, 047202 (2009).
- ¹⁴E. C. Samulon, K. A. Al-Hassanieh, Y.-J. Jo, M. C. Shapiro, L. Balicas, C. D. Batista, and I. R. Fisher, *Phys. Rev. B* **81**, 104421 (2010).
- ¹⁵X. M. Wang, C. Fan, Z. Y. Zhao, W. Tao, X. G. Liu, W. P. Ke, X. Zhao, and X. F. Sun, *Phys. Rev. B* **82**, 094405 (2010).
- ¹⁶Z. Y. Zhao, X. M. Wang, C. Fan, W. Tao, X. G. Liu, W. P. Ke, F. B. Zhang, X. Zhao, and X. F. Sun, *Phys. Rev. B* **83**, 014414 (2011).
- ¹⁷R. Berman, *Thermal Conduction in Solids* (Oxford University Press, Oxford, 1976).
- ¹⁸X. F. Sun, A. A. Taskin, X. Zhao, A. N. Lavrov, and Y. Ando, *Phys. Rev. B* **77**, 054436 (2008).
- ¹⁹X. F. Sun, I. Tsukada, T. Suzuki, S. Komiya, and Y. Ando, *Phys. Rev. B* **72**, 104501 (2005).
- ²⁰F. Heidrich-Meisner, A. Honecker, and W. Brenig, *Eur. Phys. J. Special Topics* **151**, 135 (2007).
- ²¹C. Hess, *Eur. Phys. J. Special Topics* **151**, 73 (2007).
- ²²A. V. Sologubenko, T. Lorenz, H. R. Ott, and A. Friemuth, *J. Low. Temp. Phys.* **147**, 387 (2007).
- ²³A. V. Sologubenko, K. Giannò, H. R. Ott, U. Ammerahl, and A. Revcolevschi, *Phys. Rev. Lett.* **84**, 2714 (2000).
- ²⁴E. C. Samulon, M. C. Shapiro, and I. R. Fisher, *Phys. Rev. B* **84**, 054417 (2011).
- ²⁵U. N. Upadhyaya and K. P. Sinha, *Phys. Rev.* **130**, 939 (1963).
- ²⁶R. W. White, M. Sparks, and I. Ortenburger, *Phys. Rev.* **139**, A450 (1965).